International Journal of Engineering Science 149 (2020) 103213

Contents lists available at ScienceDirect

International Journal of Engineering Science

journal homepage: www.elsevier.com/locate/ijengsci

Flexoelectricity and apparent piezoelectricity of a pantographic micro-bar

Victor A. Eremeyev [a,b,*], Jean-François Ganghoffer [c], Violetta Konopińska-Zmysłowska [a], Nikolay S. Uglov [b]

[a] Gdańsk University of Technology, ul. Gabriela Narutowicza 11/12, Gdańsk 80-233, Poland
[b] R.E. Alekseev Nizhny Novgorod Technical University, Minin St., 24, Nizhny Novgorod 603950, Russia
[c] Université de Lorraine, LEM3, UMR CNRS 7239, 7 rue Félix Savart, Metz F-57070, France

ARTICLE INFO

Article history:
Received 31 December 2019
Accepted 6 January 2020

Keywords:
Beam-lattice
Pantographic structure
Torsion
Flexoelectricity
Piezoelectricity
Effective properties

ABSTRACT

We discuss a homogenized model of a pantographic bar considering flexoelectricity. A pantographic bar consists of relatively stiff small bars connected by small soft flexoelectric pivots. As a result, an elongation of the bar relates almost to the torsion of pivots. Taking into account their flexoelectric properties we find the corresponding electric polarization. As a results, the homogenized pantographic bar demonstrates piezoelectric properties inherited from the flexoelectric properties of pivots. The effective stiffness properties of the homogenized bars are determined by the geometry of the structural elements and shear stiffness whereas the piezoelectric properties follow from the flexoelectric moduli of the pivots.

Introduction

Flexoelectricity describes a rather general property of all dielectrics. Contrary to piezoelectricity, flexoelectricity has no symmetry limitations. It is observed even for isotropic materials and materials with cubic symmetry while the piezoelectricity can only exist for materials whose crystalline point groups do not possess center of symmetry. It relates the electric polarization with strain gradients and can be observed both in solids and fluids without any symmetry limitations, see Majdoub, Sharma, and Cagin (2008), Yudin and Tagantsev (2013), Zubko, Catalan, and Tagantsev (2013), Nguyen, Mao, Yeh, Purohit, and McAlpine (2013), Wang, Gu, Zhang, and Chen (2019) and the references therein. As a result, the constitutive equations of flexoelectric solids includes strain and polarization as well as their gradients. The gradients of polarization for dielectrics were taken into account by Mindlin (1968). In a certain sense the flexoelectric continuum model can be considered as a further extension of the Toupin–Mindlin strain-gradient elasticity (Mindlin, 1964; Mindlin & Eshel, 1968; Toupin, 1962) in the case of electromagnetic media. Although a magnitude of the flexoelectricity phenomenon is rather small, it is much more pronounced at small scales, that is for micro- and nanostructured materials, as at small scales the strain gradients may be higher. So flexoelectricity is an example of so-called size-dependent phenomena. Recently flexoelectricity found

* Corresponding author at: Gdańsk University of Technology, ul. Gabriela Narutowicza 11/12, Gdańsk 80-233, Poland.
E-mail addresses: eremeyev.victor@gmail.com (V.A. Eremeyev), jean-francois.ganghoffer@univ-lorraine.fr (J.-F. Ganghoffer), violetta.konopinska@pg.edu.pl (V. Konopińska-Zmysłowska), nikolay-uglov@mail.ru (N.S. Uglov).

https://doi.org/10.1016/j.ijengsci.2020.103213

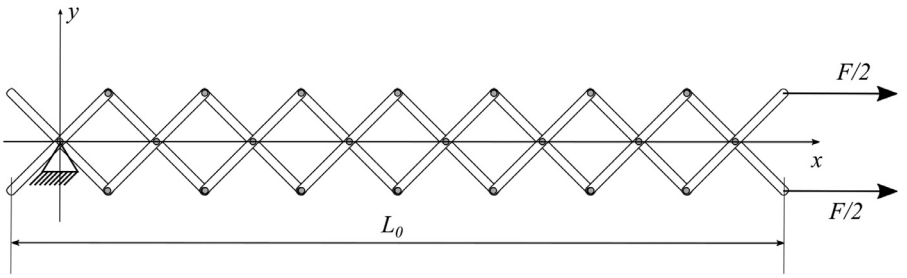

Fig. 1. Pantographic bar loaded by a net force F. The number of cells is $n = 8$.

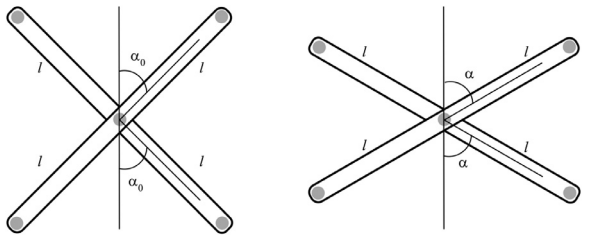

Fig. 2. Deformation of a pantographic cell.

various applications at small scales for engineering of actuators, sensors, energy harvesters and other MEMS and NEMS, see, *e.g.*, Nguyen et al. (2013), Zhang, Xu, Liu, and Shen (2015), Deng, Kammoun, Erturk, and Sharma (2014).

As flexoelectricity relates to nonhomogeneous strains, in this paper we discuss its influence on the effective properties of pantographic metamaterials. These materials constitute a particular class of beam lattices, see the review (dell'Isola et al., 2019a). A typical pantographic metamaterial consists of two families of long elastic beams connected by pivots. Torsional deformations of pivots may play a key role in the total lattice behavior, see Scerrato, Zhurba Eremeeva, Lekszycki, and Rizzi (2016), dell'Isola et al. (2019a), Spagnuolo, Peyre, and Dupuy (2019), Coutris, Thompson, and Kosaraju (2020) and the references therein. These structures were produced using 3D printing from various materials including dielectrics up to micro-meter size (dell'Isola et al., 2019b). So such micro-meter pantographic lattices may exhibit also flexoelectric properties. Here we consider a pantographic bar loaded by a net force F as shown in Fig. 1. In order to demonstrate the influence of flexoelectricity on the effective properties of the pantographic bar we restrict ourselves by consideration of rigid bars with flexoelectric pivots. So an elongation of the pantographic bar relates entirely to the torsional deformations of pivots. For nonhomogeneous strains in pivots the flexoelectricity results in appearance of an electric polarization $\mathbf{P}$. So after homogenization we get a one-dimensional (1D) piezoelectric continuum which piezoelectric properties entirely depend on flexoelectricity of the pivots.

The paper is organized as follows. First we briefly discuss the kinematics of a pantographic bar in Section 1. The pantographic bar can be treated at two scales. At the microscale we consider torsion of the flexoelectric pivots. To this end in Section 2 we recall the basic constitutive equations of flexoelectric materials. After that in Section 3 we analyze torsion of a inhomogeneous pivot and derive the corresponding energy. Finally, we treat the pantographic bar at the macroscale in Section 4. Here we discuss the effective properties of the pantographic bar treated it as an one-dimensional continuum embedded into 3D space.

In the sequel, we utilize direct (index-free) tensor calculus, vectors, second- and higher-order tensors will be denoted by boldface symbols.

1. Pantographic bar kinematics

Let us consider a pantographic structure called here a pantographic bar as shown in Fig. 1. It consists of n cells each of them consist of two rigid bars connected via elastic pivots. For n cells we have $3n - 2$ active pivots. The bar is loaded by a net force F. Considering the bar elongation we get that

$$L_0 = 2nl\sin\alpha_0, \quad L = 2nl\sin\alpha, \quad \varepsilon \equiv \frac{L - L_0}{L_0} = \frac{\sin\alpha}{\sin\alpha_0} - 1, \tag{1}$$

where L_0 and L are total lengths of the pantographic bar in the initial and deformed states, respectively, $\varepsilon_{xx} = \varepsilon$ is the strain along the pantograph, $2l$ is the length of small bars, α_0 and α are the angular variables before and after deformation as shown in Fig. 2. Obviously, being here considered as homogenized, the pantographic bar constitutes a one-dimensional (1D) continuum which possesses uniaxial tension/compression.

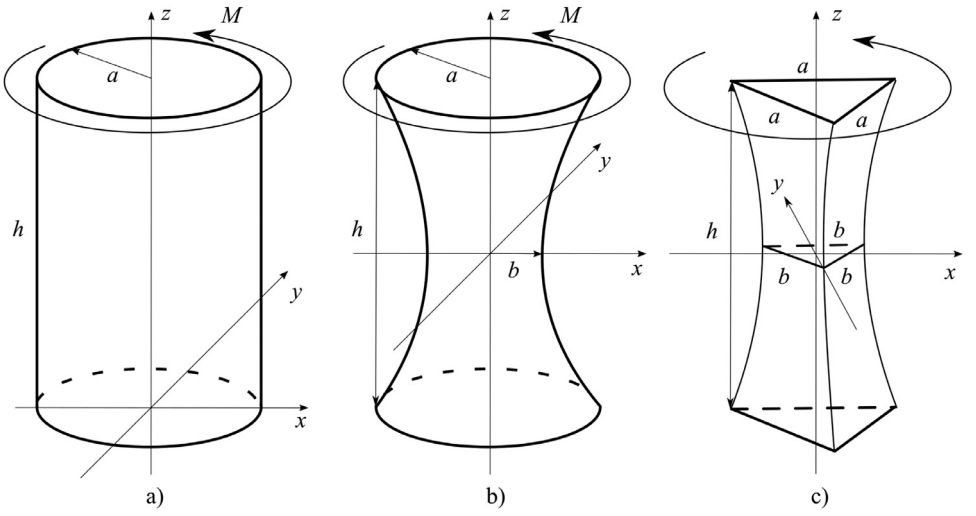

Fig. 3. Torsion of a pivot: (a) circular cylinder, $r = a$, $0 \le z \le h$; (b) circular hyperboloid, $r = (z^2 + b^2)^{1/2}$, $-h/2 \le z \le h/2$, and $a^2 = h^2/4 + b^2$; (c) solid with a triangular cross-section, which is an equilateral triangle of side length d, $d(0) = b$, $d(\pm h/2) = a$, $d(z) = b + 4(a - b)z^2/h^2$, $-h/2 \le z \le h/2$.

For small deformations we have a linear dependence between ε and $\Delta\alpha = \alpha - \alpha_0$. Indeed, linearizing (1) we get

$$L = L_0 + \Delta L, \quad \Delta L = 2nl\varepsilon\,\Delta\alpha, \quad \varepsilon = \cot\alpha_0\,\Delta\alpha. \tag{2}$$

Similarly, the transverse strain is given by the relation $\varepsilon_{yy} = -\tan\alpha_0\,\Delta\alpha = -\tan^2\alpha_0\,\varepsilon$. As a mechanical model of pivots we consider the linear dependence of the total torque M on the twist τ

$$M = \mathbb{K}\tau, \tag{3}$$

where $\mathbb{K}$ is a torsional stiffness whereas $\tau = 2\Delta\alpha$. If we consider the pivot as an elastic circular cylinder of height h and of radius a, see Fig. 3(a), the elementary theory of torsion results in the following formula, see, *e.g.*, (Timoshenko and Goodier, 1951, p. 264)

$$\mathbb{K} = \mu J_p/h, \tag{4}$$

where μ is a shear modulus and $J_p = \pi a^4/2$ is the polar moment of inertia.

In this case the total strain energy stored in all pivots is given by

$$\mathcal{E}_t = 2(3n-2)\mathbb{K}(\Delta\alpha)^2 = 2(3n-2)\frac{\mathbb{K}}{(\cot\alpha_0)^2}\varepsilon^2. \tag{5}$$

The equilibrium condition of the pantographic bar follows from the variational equation

$$\delta\mathcal{E}_t - \delta\mathcal{A} = 0, \tag{6}$$

where $\mathcal{A} = F(L - L_0)$ is the work of the external force and δ is the symbol of variation. From (6) we get that

$$\varepsilon = \frac{n}{3n-2}\frac{Fl}{2\mathbb{K}}\sin\alpha_0.$$

Obviously, the last formula gives the expression for the effective extensional stiffness of the pantographic bar

$$\mathbb{E} = 2\frac{3n-2}{nl\sin\alpha_0}\mathbb{K}. \tag{7}$$

In the following we analyze the influence of the microscopic flexoelectricity existing within the pantographic unit cell on its effective piezoelectric properties.

2. Basic relations of flexoelectricity

In order to consider the deformations of the pantographic bar at the microscale we study torsional deformations of flexoelectric pivots. First, following Majdoub et al. (2008) let us briefly recall the basic equations of the flexoelectricity. In what follows we restrict ourselves to infinitesimal deformations. In the theory we introduce the following primary variables

$$\mathbf{u} = \mathbf{u}(\mathbf{x}, t), \quad \mathbf{P} = \mathbf{P}(\mathbf{x}, t), \tag{8}$$

where $\mathbf{u}$ and $\mathbf{P}$ are vectors of displacements and electric polarization, respectively, $\mathbf{x}$ is the position vector, and t is time. Here we restrict to the pure electromechanical theory, so the energy density takes the form

$$W = W(\boldsymbol{\varepsilon}, \mathbf{P}, \nabla\nabla\mathbf{u}, \nabla\mathbf{P}), \qquad \boldsymbol{\varepsilon} = \frac{1}{2}\left(\nabla\mathbf{u} + (\nabla\mathbf{u})^T\right), \tag{9}$$

where $\boldsymbol{\varepsilon}$ is the strain tensor and ∇ denotes the three-dimensional nabla-operator. If we neglect the dependence on $\mathbf{P}$ and $\nabla\mathbf{P}$ in (9) we recover the Toupin–Mindlin strain gradient elasticity (Mindlin, 1964; Mindlin & Eshel, 1968; Toupin, 1962). On the other hand, if we omit in (9) only second deformation gradient $\nabla\nabla\mathbf{u}$ we get Mindlin's theory of dielectrics (Mindlin, 1968). Finally, Eq. (9) can be reduced to the piezoelectricity with constitutive equation encapsulated by the following form of the energy density (Eringen & Maugin, 1990; Maugin, 2017):

$$W = W(\boldsymbol{\varepsilon}, \mathbf{P}).$$

For flexoelectric solids the equations of equilibrium can be derived from the variational principle (Majdoub et al., 2008; Nguyen et al., 2013)

$$\delta \int_V (W - \frac{1}{2}\epsilon_0 \mathbf{E}\cdot\mathbf{E} - \mathbf{P}\cdot\mathbf{E})\, dV = 0, \tag{10}$$

where for brevity we omitted all external actions, V is a volume which is occupied by the solid body, ϵ_0 is a vacuum permittivity, $\cdot$ is the dot product, and $\mathbf{E}$ is the electric field, which can be expressed through the electric potential ϕ as follows

$$\mathbf{E} = -\nabla\phi.$$

Last relation ensures that Maxwell's equation

$$\nabla \times \mathbf{E} = \mathbf{0}, \tag{11}$$

is automatically satisfied. Here $\times$ denotes the cross product. As a result, from (10) we get the equilibrium equation

$$\nabla\cdot\boldsymbol{\sigma} = \mathbf{0}, \quad \boldsymbol{\sigma} = \mathbf{T} - \nabla\cdot\mathbf{M}, \quad \mathbf{T} = \frac{\partial W}{\partial \boldsymbol{\varepsilon}}, \quad \mathbf{M} = \frac{\partial W}{\partial \nabla\nabla\mathbf{u}}, \tag{12}$$

and

$$\nabla\cdot\mathbf{D} = 0, \quad \mathbf{D} = \epsilon_0\mathbf{E} + \mathbf{P}, \tag{13}$$

$$\mathbf{E} \equiv -\nabla\phi = \frac{\partial W}{\partial \mathbf{P}} - \nabla\cdot\frac{\partial W}{\partial \nabla\mathbf{P}}, \tag{14}$$

in the domain V with proper boundary conditions, see Majdoub et al. (2008). Here $\boldsymbol{\sigma}$ is the total stress tensor, $\mathbf{T}$ and $\mathbf{M}$ are the stress and hyper-stress tensors, respectively, and $\mathbf{D}$ is the electric displacement field. Eq. (13) is another Maxwell's equation of electrostatics, see Eringen and Maugin (1990) and Maugin (2017).

In what follows we consider W as a quadratic form of its arguments

$$W = \frac{1}{2}\boldsymbol{\varepsilon} : \mathbf{C} : \boldsymbol{\varepsilon} + \frac{1}{2}\mathbf{P}\cdot\mathbf{A}\cdot\mathbf{P} - \mathbf{P}\cdot\mathbf{d} : \boldsymbol{\varepsilon} + \frac{1}{2}\nabla\mathbf{P} : \mathbf{B} : \nabla\mathbf{P} - \nabla\boldsymbol{\varepsilon}\vdots\mathbf{F}\cdot\mathbf{P} - \boldsymbol{\varepsilon} : \mathbf{H} : \nabla\mathbf{P} + \frac{1}{2}\nabla\nabla\mathbf{u}\vdots\mathbf{G}\vdots\nabla\nabla\mathbf{u}, \tag{15}$$

where : and $\vdots$ stand for double and triple dot products, respectively, and several material tensors are introduced. In (15), $\mathbf{C}$ is a fourth-order tensor of elastic moduli, $\mathbf{A} = \boldsymbol{\chi}^{-1}$ is a symmetric second-order reciprocal dielectric susceptibility tensor, $\mathbf{d}$ is a third–order piezoelectric tensor, $\mathbf{B}$ is a polarization gradient coupling fourth-order tensor, $\mathbf{F}$ and $\mathbf{H}$ denote fourth-order flexocoupling tensors, and $\mathbf{G}$ is a six-order tensor of elastic moduli related to strain-gradients. In the literature one can find different and even more complex forms of stored energy functions, see *e.g.* Yudin and Tagantsev (2013) and Wang et al. (2019). The components of $\mathbf{C}$ have standard symmetry restrictions $C_{ijmn} = C_{mnij} = C_{jimn}$, other tensors also have symmetry properties: $d_{ijk} = d_{jik}$, $B_{ijmn} = B_{mnij}$, $F_{ijmn} = F_{jimn}$, etc., see Olive and Auffray (2014) and Auffray, He, and Quang (2019) for further details. Flexocoupling tensors $\mathbf{F}$ and $\mathbf{H}$ are mutually dependent, see Yudin and Tagantsev (2013) and Wang et al. (2019).

From (15) we get the dependence for stress tensor

$$\mathbf{T} = \mathbf{C} : \boldsymbol{\varepsilon} - \mathbf{P}\cdot\mathbf{d} - (\mathbf{H} : \nabla\mathbf{P})^T. \tag{16}$$

Obviously, $\mathbf{T}$ depends on polarization and its gradient. Using the relations

$$\frac{\partial W}{\partial \mathbf{P}} = \mathbf{A}\cdot\mathbf{P} - \mathbf{d} : \boldsymbol{\varepsilon} - \nabla\boldsymbol{\varepsilon}\vdots\mathbf{F}, \quad \frac{\partial W}{\partial \nabla\mathbf{P}} = \mathbf{B} : \nabla\mathbf{P} - \boldsymbol{\varepsilon} : \mathbf{H}, \tag{17}$$

Eq. (14) transforms into

$$\mathbf{E} = \mathbf{A}\cdot\mathbf{P} - \mathbf{d} : \boldsymbol{\varepsilon} - \nabla\boldsymbol{\varepsilon}\vdots\mathbf{F} - \nabla\cdot(\mathbf{B} : \nabla\mathbf{P}) + \nabla\cdot(\boldsymbol{\varepsilon} : \mathbf{H}). \tag{18}$$

In the case of homogeneous materials and when the polarization gradient is constant from (18) we get the key equation of flexoelectricity

$$\mathbf{P} = \boldsymbol{\chi} \cdot \mathbf{E} + \mathbf{e} : \boldsymbol{\varepsilon} + \boldsymbol{\mu} \dot{:} \nabla \boldsymbol{\varepsilon}, \tag{19}$$

which establishes a linear dependence between the polarization and strain gradients with the fourth-order flexoelectric tensor $\boldsymbol{\mu}$ defined though the relation

$$\boldsymbol{\mu} \dot{:} \nabla \boldsymbol{\varepsilon} = \boldsymbol{\chi} \cdot [\nabla \boldsymbol{\varepsilon} \dot{:} \mathbf{F} - \nabla \cdot (\boldsymbol{\varepsilon} : \mathbf{H})] \quad \forall \boldsymbol{\varepsilon},$$

see Yudin and Tagantsev (2013) and Wang et al. (2019), wherein we also introduced another piezoelectric tensor $\mathbf{e} = \boldsymbol{\chi} \cdot \mathbf{d}$. Without electric field and for non-piezoelectric materials, that is when $\mathbf{d} = \mathbf{0}$, Eq. (19) reduces to

$$\mathbf{P} = \boldsymbol{\mu} \dot{:} \nabla \boldsymbol{\varepsilon}. \tag{20}$$

Eqs. (19) and (20) give also the possibility to introduce $\mathbf{e}$ and $\boldsymbol{\mu}$ as follows

$$\mathbf{e} = \frac{\partial \mathbf{P}}{\partial \boldsymbol{\varepsilon}}, \quad \boldsymbol{\mu} = \frac{\partial \mathbf{P}}{\partial \nabla \boldsymbol{\varepsilon}}, \tag{21}$$

see Yudin and Tagantsev (2013) and Wang et al. (2019) for details.

Symmetry restrictions for flexoelectric tensors are studied by Le Quang and He (2011). For materials with cubic symmetry there exist only three independent components of $\boldsymbol{\mu}$ that are μ_{1111}, μ_{1122}, and μ_{1212} (this holds in the present 2D context). Using matrix notations $\boldsymbol{\mu}$ can be written as (Nguyen et al., 2013)

$$\boldsymbol{\mu} = \begin{pmatrix} \mu_{11} & \mu_{12} & \mu_{12} & 0 & 0 & 0 \\ \mu_{12} & \mu_{11} & \mu_{12} & 0 & 0 & 0 \\ \mu_{12} & \mu_{12} & \mu_{11} & 0 & 0 & 0 \\ 0 & 0 & 0 & \mu_{44} & 0 & 0 \\ 0 & 0 & 0 & 0 & \mu_{44} & 0 \\ 0 & 0 & 0 & 0 & 0 & \mu_{44} \end{pmatrix}, \tag{22}$$

where $\mu_{11} = \mu_{1111}$, $\mu_{12} = \mu_{1122}$, and $\mu_{44} = \mu_{1212}$. For isotropic materials $\boldsymbol{\mu}$ takes the form (Le Quang & He, 2011)

$$\boldsymbol{\mu} = \mu_{ijkl} \mathbf{e}_i \otimes \mathbf{e}_j \otimes \mathbf{e}_k \otimes \mathbf{e}_l,$$

where

$$\mu_{ijkl} = \mu_1(\delta_{ik}\delta_{lj} + \delta_{il}\delta_{kj} + \delta_{ij}\delta_{kl}) + \mu_2(\delta_{ik}\delta_{lj} + \delta_{il}\delta_{kj} - 2\delta_{ij}\delta_{kl}), \tag{23}$$

μ_1 and μ_2 are two independent flexoelectric moduli, and δ_{ij} is the Kronecker symbol.

Neglecting flexoelectric and strain gradient contributions we come to the constitutive equations of piezoelectric solids

$$W = W(\boldsymbol{\varepsilon}, \mathbf{P}) = \frac{1}{2}\boldsymbol{\varepsilon} : \mathbf{C} : \boldsymbol{\varepsilon} + \frac{1}{2}\mathbf{P} \cdot \mathbf{A} \cdot \mathbf{P} - \mathbf{P} \cdot \mathbf{d} : \boldsymbol{\varepsilon}, \tag{24}$$

which entails

$$\boldsymbol{\sigma} = \mathbf{T} = \mathbf{C} : \boldsymbol{\varepsilon} - \mathbf{P} \cdot \mathbf{d}, \quad \mathbf{E} = \mathbf{A} \cdot \mathbf{P} - \mathbf{d} : \boldsymbol{\varepsilon}. \tag{25}$$

Eq. (25) $_2$ can be written also as

$$\mathbf{P} = \boldsymbol{\chi} \cdot \mathbf{E} + \mathbf{e} : \boldsymbol{\varepsilon}. \tag{26}$$

In what follows we use these constitutive equations at the macroscale in Section 4.

3. Torsion

As pivots of the pantographic bar are subjected to torsional deformations let us consider the torsion of a flexoelectric cylinder treated as a model of the pivot, see Fig. 3. The solution of the corresponding boundary-value problem for a flexoelectric cylinder constitutes a rather complex coupled problem for displacements and electric potential. Instead, here we utilize an approximated solution following from the elementary theory of torsion (Timoshenko & Goodier, 1951). From the theory of torsion we will get strain $\boldsymbol{\varepsilon}$, then its gradient and using (20) we estimate $\mathbf{P}$. Similar estimation was also used by Zhang et al. (2015).

First, let us consider a Saint–Venant-type solution for a circular cylinder

$$\mathbf{u} = \theta(z)\mathbf{e}_z \times \mathbf{x}, \quad \theta(z) = \theta_0 z, \tag{27}$$

where r, φ, z are the polar coordinates and $\mathbf{e}_r$, $\mathbf{e}_\varphi$ and $\mathbf{e}_z$ are corresponding unit base vectors, and $\theta_0 = \tau/h$ is a twist angle per unit length. So here we have that

$$\nabla \mathbf{u} = \theta_0 \mathbf{e}_z \otimes \mathbf{e}_z \times \mathbf{x} - \theta_0 z \mathbf{I} \times \mathbf{e}_z, \quad \boldsymbol{\varepsilon} = \gamma r(\mathbf{e}_z \otimes \mathbf{e}_\varphi + \mathbf{e}_\varphi \otimes \mathbf{e}_z), \qquad \gamma = \frac{1}{2}\theta_0,$$

where $\otimes$ is the dyadic product. Obviously, here $\nabla\boldsymbol{\varepsilon} \neq \boldsymbol{0}$ as $\boldsymbol{\varepsilon}$ is a linear function of r. It is given by

$$\nabla\boldsymbol{\varepsilon} = \gamma\left(\mathbf{e}_r \otimes \mathbf{e}_z \otimes \mathbf{e}_\varphi + \mathbf{e}_r \otimes \mathbf{e}_\varphi \otimes \mathbf{e}_z - \mathbf{e}_\varphi \otimes \mathbf{e}_z \otimes \mathbf{e}_r - \mathbf{e}_\varphi \otimes \mathbf{e}_r \otimes \mathbf{e}_z\right).$$

Nevertheless, using (20) and (22) we get that $\mathbf{P} = \mathbf{0}$. So no polarization is induced by the strain gradient term, thus flexoelectric effects do not appear for the effective homogenized pantograph. For a circular cylinder the flexoelectric effect should be expected for less symmetrical constitutive equations.

The situation is completely different if we consider a circular cylinder with variable diameter as the circular hyperboloid shown in Fig. 3(b). Even in the case of pure linear elasticity this problem requires a rather complex technique, see Neuber (1946). In the following we use the semi-inverse method: we assume the solution again in the form (27) with z-dependent twist:

$$\mathbf{u} = \theta(z)\mathbf{e}_z \times \mathbf{x}, \tag{28}$$

where for $\theta(z)$ we use the formula

$$\theta(z) = \int_{-h/2}^{z} \frac{M}{\mu J_p(\xi)}\, d\xi, \tag{29}$$

and $J_p(z) = \pi r^4(z)/2$ is the polar moment of inertia and $r(z) = (z^2 + b^2)^{1/2}$ is the equation of the pivot surface (Fig. 3(b)). Obviously, for constant J_p we recover the previous case with a linear dependence $\theta = \theta_0 z$. Here we get

$$\boldsymbol{\varepsilon} = \gamma r(\mathbf{e}_z \otimes \mathbf{e}_\varphi + \mathbf{e}_\varphi \otimes \mathbf{e}_z), \qquad \gamma = \frac{1}{2}\theta', \tag{30}$$

$$\nabla\boldsymbol{\varepsilon} = \gamma' r\left(\mathbf{e}_z \otimes \mathbf{e}_z \otimes \mathbf{e}_\varphi + \mathbf{e}_z \otimes \mathbf{e}_\varphi \otimes \mathbf{e}_z\right) + \gamma\left(\mathbf{e}_r \otimes \mathbf{e}_z \otimes \mathbf{e}_\varphi + \mathbf{e}_r \otimes \mathbf{e}_\varphi \otimes \mathbf{e}_z - \mathbf{e}_\varphi \otimes \mathbf{e}_z \otimes \mathbf{e}_r - \mathbf{e}_\varphi \otimes \mathbf{e}_r \otimes \mathbf{e}_z\right). \tag{31}$$

Hereafter the prime stands for the derivative with respect to z. With (31) and using (20) and (22) we have

$$\mathbf{P} = (\mu_{1122} + \mu_{1212})\gamma' r\mathbf{e}_\varphi. \tag{32}$$

Similarly, using (23) we get for an isotropic solid

$$\mathbf{P} = 2(\mu_1 + \mu_2)\gamma' r\mathbf{e}_\varphi. \tag{33}$$

In other words, unlike the previous case we get here the flexoelectric effect for isotropic materials and materials with cubic symmetry. Nevertheless, for (32) and (33) the mean polarization is zero:

$$\tilde{\mathbf{P}} \equiv \langle \mathbf{P} \rangle \equiv \frac{1}{V}\int_V \mathbf{P}\, dV = \mathbf{0}, \tag{34}$$

where V is the volume of the pivot. On the other hand, the flexoelectric contribution in the energy is not zero. Indeed, the flexoelectric contribution given by

$$W_{flexo} = \frac{1}{2}\nabla\mathbf{P} : \mathbf{B} : \nabla\mathbf{P} - \nabla\boldsymbol{\varepsilon}\vdots\mathbf{F}\cdot\mathbf{P} - \boldsymbol{\varepsilon} : \mathbf{H} : \nabla\mathbf{P} \tag{35}$$

does not vanish after averaging, in general.

Both considered above examples possess a certain symmetry of the cross-section. Now let us consider less symmetric pivots. As an example we analyze a pivot with triangular cross-section, see Fig. 3(c). Here the cross-section has a form of the equilateral triangle of side length $d = d(z)$. Unlike previous cases, here the displacement field is not planar (Timoshenko & Goodier, 1951). We assume a solution in the form

$$\mathbf{u} = \theta(z)\mathbf{e}_z \times \mathbf{x} + \psi(x, y, z)\mathbf{e}_z, \tag{36}$$

where $\psi(x, y, z)$ is an unknown function. In the case of constant side d, ψ has a form

$$\psi = \theta_0\eta(x, y),$$

where $\eta(x, y)$ is the warping (torsion) function and θ_0 is the twist per unit length (Timoshenko & Goodier, 1951). For the equilateral triangle of side d, η is given by

$$\eta(x, y) = \frac{y(3x^2 - y^2)}{6d},$$

whereas the torsional stiffness is $\mathbb{K} = \sqrt{3}\mu d^4/80h$, see (Landau & Lifshitz, 1970, p. 74). In the following we consider the approximate solution with ψ given by

$$\psi = \theta'(z)\frac{y(3x^2 - y^2)}{6d(z)}, \tag{37}$$

where $\theta(z)$ is given by (29) with $J_p = \frac{\sqrt{3}d^4(z)}{48}$.

Calculations of $\boldsymbol{\varepsilon}$ and $\nabla\boldsymbol{\varepsilon}$ leads to awkward formulae which we omit for brevity. Here $\nabla\boldsymbol{\varepsilon}$ includes the term

$$\psi''\mathbf{e}_z\otimes\mathbf{e}_z\otimes\mathbf{e}_z.$$

With (23) it produces the transverse polarization

$$P_3 = 3\mu_1\psi''. \tag{38}$$

Here the mean polarization does not vanish and it is given by

$$\bar{\mathbf{P}} \equiv \langle\mathbf{P}\rangle = \bar{P}_3\mathbf{e}_z, \qquad \bar{P}_3 = 3\mu_1\frac{1}{V}\int_V \psi''\,dx\,dy\,dz. \tag{39}$$

The discussed above three examples of the pivots confirm the conclusion by Sharma, Maranganti, and Sharma (2007): the effective piezoelectricity requires some constraints on non-centrosymmetry of flexoelectric composites. More precisely, the microstructure should break centrosymmetry. The first example is the most symmetric one, so for an isotropic solid we have not flexoelectricity effect. For the second example we get polarization at the microscale but it disappears after averaging. As a third example the mean polarization does not vanish, it presents a case which exactly corresponds to the requirement of violation of centrosymmetry and could be a good candidate for effective piezoelectric composites.

4. Effective piezoelectric properties of the pantograph

Let us consider macroscopic deformations of the pantograph with triangular pivots. In order to demonstrate the flexoelectricity influence at the macroscale let us consider a pure isotropic dielectric, that is when $\mathbf{d}=\mathbf{0}$, $\mathbf{A}=\chi_0^{-1}\mathbf{I}$. Here $\mathbf{I}$ is the unit 3D tensor and χ_0 is the dielectric susceptibility. In addition we neglect also strain gradient properties: $\mathbf{G}=\mathbf{0}$. So Eq. (15) takes the form

$$W = \frac{1}{2}\boldsymbol{\varepsilon}:\mathbf{C}:\boldsymbol{\varepsilon} + \frac{1}{2}\chi_0^{-1}\mathbf{P}\cdot\mathbf{P} + W_{flexo}, \tag{40}$$

where W_{flexo} is given by (35). Note that here $\mathbf{C}$ is an isotropic fourth-order tensor with two Lamé moduli λ and μ.

Considering the pantographic bar at the macroscale we introduce the longitudinal strain ε defined in $(1)_3$. Obviously, an elongation/compression of the bar results in affine deformations, so ε does not depend on the coordinates x, y, and $\nabla\varepsilon=0$. Thus, at the macroscale the here considered pantographic bar behaves as a Cauchy continuum. Note that this conclusion fails if we relax the requirement of rigidity of the small bars in the pantograph, see (dell'Isola et al., 2019a). Moreover, the homogenization of pantographic structures with flexible structural elements results in various enhanced models of continuum, see, *e.g.*, Rahali, Giorgio, Ganghoffer, and dell'Isola (2015) and Abdoul-Anziz and Seppecher (2018).

The polarization at the macroscale is a result of averaging given by (39). Note that $\bar{\mathbf{P}}$ is also constant, that it does not depend on macroscopic coordinates. So the possible dependence $\bar{\mathbf{P}}$ on ε is linear as for a piezoelectric material (26) with $\mathbf{E}=\mathbf{0}$. Let us find the dependence $\bar{\mathbf{P}}$ on ε. The macroscopic strain ε can be related to microscopic solutions for the pivots as follows. Using Eqs. $(2)_3$ and (3) we get

$$M = 2\mathbb{K}\tan\alpha_0\,\varepsilon.$$

Then, from (29) it follows that

$$\theta(z) = \frac{2\mathbb{K}\tan\alpha_0}{\mu}\int_{-h/2}^{z}\frac{d\xi}{J_p(\xi)}\,\varepsilon, \quad \psi(x,y,z) = \frac{\mathbb{K}\tan\alpha_0}{3\mu J_p(z)d(z)}y(3x^2-y^2)\,\varepsilon. \tag{41}$$

Using (26) and $(41)_2$ we obtain that

$$\bar{P}_3 = e_{311}\varepsilon \tag{42}$$

with the effective piezoelectric modulus e_{311} given by

$$e_{311} = \mu_1\frac{\mathbb{K}\tan\alpha_0}{\mu V}\int_V\frac{d^2}{dz^2}\frac{y(3x^2-y^2)}{J_p(z)d(z)}\,dx\,dy\,dz. \tag{43}$$

In order to extend the equilibrium conditions for the homogenized model of the pantographic bar presented in Section 1 let us consider the total energy functional. As we have $3n-2$ active pivots for the pantographic bar, we get that the total energy has the form

$$\mathcal{E} = \mathcal{E}_t + \mathcal{E}_p + \mathcal{E}_e, \tag{44}$$

where $\mathcal{E}_t$ is given by (5), $\mathcal{E}_p$ is the flexoelectric contribution given by the formula

$$\mathcal{E}_p = (3n-2)\int_V W_{flexo}\,dx\,dy\,dz, \quad \mathcal{E}_e = (3n-2)V\chi_0^{-1}\bar{P}_3^2. \tag{45}$$

So in addition, for $\mathbf{E}=\mathbf{0}$ and using the variational equation $\delta\mathcal{E}-\delta\mathcal{A}=0$ one can get a modification of an effective elastic stiffness $\mathbb{E}$ due to the mean polarization.

Let us summarize our assumptions and future possible steps towards further modelling of the flexoelectric pantographs.

1. Here we used approximated analytical approach to the torsion analysis. The exact solution of the coupled problem of torsion of flexoelectric prismatic solids can be given.
2. Considering torsion we neglected strain-gradient in the energy assuming $\mathbf{G} = \mathbf{0}$. On the other hand for $\mathbf{G} \neq 0$ we have size-dependence which could be important at small scales, see, *e.g.*, Cordero, Forest, and Busso (2016). Moreover, by definition for strain-gradient elasticity we get solutions with gradients of strains such as boundary-layer type solutions, which result in flexoelectric effect. So one can expect that within the strain gradient elasticity we have more pronounced flexoelectricity.
3. A pantographic structure itself may be considered as a strain-gradient continuum if we take into account the bending of bars constituting the pantograph (dell'Isola et al., 2019a; Rahali et al., 2015). Let us note that bending is also related to flexoelectricity (Nguyen et al., 2013; Wang et al., 2019). So it is seen that we have a deep correlation of deformations of the pantographs with flexoelectricity which may result in upscaling of flexoelectricity at the microscale into piezoelectricity at the macroscale.
4. At small scales the surface piezoelectricity and surface flexoelectricity may significantly improve the coupling between strain gradients and polarization (Yudin & Tagantsev, 2013; Yurkov & Tagantsev, 2016). As pantographs have high surface-to-volume ratio, such surface-enhanced models may provide the increase of the piezoelectricity at the macroscale.
5. As we can see considering various shapes of pivots, when modelling flexoelectric pantographs one should pay a particular attention to the optimal choice of the microgeometry in order to improve the effective piezoelectricity.

5. Conclusions

Considering relatively simple example of a microstructured material such as a pantographic bar, we have been illustrated that such general phenomenon as flexoelectricity may result in the appearance of piezoelectric properties at the macroscale for properly chosen microstructure. Here the homogenized 1D continuum possesses piezoelectricity with some effective properties inherited from the geometrical and flexoelectric properties of pivots. This example demonstrates that the flexoelectricity for a beam-lattice with dominant bending or/and shear deformations may significantly improve a piezoelectric response as in the case of thin films (Lee & Noh, 2012; Majdoub, Sharma, & Cagin, 2008; Nguyen, Mao, Yeh, Purohit, & McAlpine, 2013; Sharma, Maranganti, & Sharma, 2007). In a certain sense the discussed effect is similar to surface-related phenomena for media with high surface-to-volume ratio as discussed by Yurkov and Tagantsev (2016) and Liu, Wu, and Wang (2016). As the recent period witnesses a significant progress in additive technologies, it can be used for optimal design of perspective piezoelectric and flexoelectric nanocomposites. Moreover, due to its high flexibility the discussed pantographic bar could be used as a working element of MEMS.

Acknowledgments

V.A.E. and N.S.U. acknowledge the support by grant 14.Z50.31.0036 awarded to R. E. Alekseev Nizhny Novgorod Technical University by Department of Education and Science of the Russian Federation. V.A.E. is also thankful to the Université de Lorraine (France) and the Laboratoire LEM3 for the support and hospitality during his visit in December 2019 where work on this paper was completed.

References

Abdoul-Anziz, H., & Seppecher, P. (2018). Strain gradient and generalized continua obtained by homogenizing frame lattices. *Mathematics and Mechanics of Complex Systems, 6*(3), 213–250.

Auffray, N., He, Q. C., & Quang, H. L. (2019). Complete symmetry classification and compact matrix representations for 3D strain gradient elasticity. *International Journal of Solids and Structures, 159*, 197–210.

Cordero, N. M., Forest, S., & Busso, E. P. (2016). Second strain gradient elasticity of nano-objects. *Journal of Mechanics and Physics of Solids, 97*, 92–124.

Coutris, N., Thompson, L. L., & Kosaraju, S. (2020). Asymptotic homogenization models for pantographic lattices with variable order rotational resistance at pivots. *Journal of the Mechanics and Physics of Solids, 134*, 103718.

dell'Isola, F., Seppecher, P., Spagnuolo, M., Barchiesi, E., Hild, F., Lekszycki, T., et al. (2019a). Advances in pantographic structures: design, manufacturing, models, experiments and image analyses. *Continuum Mechanics and Thermodynamics, 31*(4), 1231–1282.

dell'Isola, F., Turco, E., Misra, A., Vangelatos, Z., Grigoropoulos, C., & Melissinaki, V. (2019b). Force–displacement relationship in micro-metric pantographs: Experiments and numerical simulations. *Comptes Rendus Mécanique, 347*(5), 397–405.

Deng, Q., Kammoun, M., Erturk, A., & Sharma, P. (2014). Nanoscale flexoelectric energy harvesting. *International Journal of Solids and Structures, 51*(18), 3218–3225.

Eringen, A. C., & Maugin, G. A. (1990). *Electrodynamics of continua*. New York: Springer.

Landau, L. D., & Lifshitz, E. M. (1970). Theory and elasticity. *Course of theoretical physics*: 7 (2nd Ed). Oxford: Pergamon Press.

Le Quang, H., & He, Q. C. (2011). The number and types of all possible rotational symmetries for flexoelectric tensors. *Proceedings of the Royal Society A: Mathematical, Physical and Engineering Sciences, 467*(2132), 2369–2386.

Lee, D., & Noh, T. W. (2012). Giant flexoelectric effect through interfacial strain relaxation. *Philosophical Transactions of the Royal Society A: Mathematical, Physical and Engineering Sciences, 370*(1977), 4944–4957.

Liu, C., Wu, H., & Wang, J. (2016). Giant piezoelectric response in piezoelectric/dielectric superlattices due to flexoelectric effect. *Applied Physics Letters, 109*(19), 192901.

Majdoub, M. S., Sharma, P., & Cagin, T. (2008). Enhanced size-dependent piezoelectricity and elasticity in nanostructures due to the flexoelectric effect. *Physical Review B, 77*(12), 125424.

Maugin, G. A. (2017). *Non-classical continuum mechanics: A dictionary*. Singapore: Springer.
Mindlin, R. D. (1964). Micro-structure in linear elasticity. *Archive for Rational Mechanics and Analysis, 16*(1), 51–78.
Mindlin, R. D. (1968). Polarization gradient in elastic dielectrics. *International Journal of Solids and Structures, 4*(6), 637–642.
Mindlin, R. D., & Eshel, N. N. (1968). On first strain-gradient theories in linear elasticity. *International Journal of Solids and Structures, 4*(1), 109–124.
Neuber, H. (1946). *Theory of notch stresses: Principles for exact stress calculation*. Ann Arbor, Michigan: JW Edwards.
Nguyen, T. D., Mao, S., Yeh, Y.-W., Purohit, P. K., & McAlpine, M. C. (2013). Nanoscale flexoelectricity. *Advanced Materials, 25*(7), 946–974.
Olive, M., & Auffray, N. (2014). Symmetry classes for odd-order tensors. *ZAMM, 94*(5), 421–447.
Rahali, Y., Giorgio, I., Ganghoffer, J., & dell'Isola, F. (2015). Homogenization à la Piola produces second gradient continuum models for linear pantographic lattices. *International Journal of Engineering Science, 97*, 148–172.
Scerrato, D., Zhurba Eremeeva, I. A., Lekszycki, T., & Rizzi, N. L. (2016). On the effect of shear stiffness on the plane deformation of linear second gradient pantographic sheets. *ZAMM, 96*(11), 1268–1279.
Sharma, N. D., Maranganti, R., & Sharma, P. (2007). On the possibility of piezoelectric nanocomposites without using piezoelectric materials. *Journal of the Mechanics and Physics of Solids, 55*(11), 2328–2350.
Spagnuolo, M., Peyre, P., & Dupuy, C. (2019). Phenomenological aspects of quasi-perfect pivots in metallic pantographic structures. *Mechanics Research Communications, 101*, 103415.
Timoshenko, S., & Goodier, J. N. (1951). *Theory of elasticity* (2nd Ed). New York: McGraw-Hill.
Toupin, R. A. (1962). Elastic materials with couple-stresses. *Arch Ration Mech Analysis, 11*(1), 385–414.
Wang, B., Gu, Y., Zhang, S., & Chen, L.-Q. (2019). Flexoelectricity in solids: Progress, challenges, and perspectives. *Progress in Materials Science, 106*, 100570.
Yudin, P. V., & Tagantsev, A. K. (2013). Fundamentals of flexoelectricity in solids. *Nanotechnology, 24*(43), 432001.
Yurkov, A. S., & Tagantsev, A. K. (2016). Strong surface effect on direct bulk flexoelectric response in solids. *Applied Physics Letters, 108*(2), 022904.
Zhang, S., Xu, M., Liu, K., & Shen, S. (2015). A flexoelectricity effect-based sensor for direct torque measurement. *Journal of Physics D: Applied Physics, 48*(48), 485502.
Zubko, P., Catalan, G., & Tagantsev, A. K. (2013). Flexoelectric effect in solids. *Annual Review of Materials Research, 43*(1), 387–421.